Acta Crystallographica Section A
Foundations of Crystallography
ISSN 0108-7673

Received 17 June 2008
Accepted 26 September 2008

Detection and characterization of ultra-thin films with neutron reflectometry

Z. Tun

Canadian Neutron Beam Centre, National Research Council Canada, Chalk River, Ontario, Canada. Correspondence e-mail: zin.tun@nrc.gc.ca

Specular reflectometry, being a technique based on interference between coherent X-ray or neutron beams, is considered to have a fundamental limit in sensing the presence of films that are too thin for the maximum momentum transfer, Q_{max}, to which reflectivity has been measured. However, it is known both experimentally and from simulations that an ultra-thin film, with thickness $t << 2\pi/Q_{max}$, can be detected if it exists sandwiched between two contrast-matched media. This possibility is qualitatively explained using phase-vector diagrams. The diagrams also show that the detection is through unmistakable shifts of the interference maxima and minima, and that the scattering-length density of the ultra-thin film determined by least-squares analysis is unique.

1. Introduction

The specular reflectivity from a single flat interface as a function of scattering wavevector, Q, perpendicular to the interface is given by Fresnel's equation. The reflectivity is unity from $Q = 0$ to Q_c, the critical wavevector for total external (or internal) reflection, followed by a rapid monotonic decline for wavevectors beyond Q_c. In the case of parallel stratified layers with more than a single interface, intensity modulations known as Kiessig fringes are observed. The modulations may be of single periodicity or a superposition of several periodicities, depending on whether the sample consists, respectively, of two or more than two interfaces. Indeed, it is through these periodicities that the least-squares analysis of the reflectometry data determines the thickness and other characteristics of the layers.

The above reasoning implies that the magnitude of the highest Q to which reflectivity has been measured will impose a fundamental limit on the thinnest layer one could detect and investigate with reflectometry. If we define $t_{min} \equiv 2\pi/Q_{max}$, a layer of thickness $\geq t_{min}$ would have contributed at least one cycle of constructive/destructive interference in a scan from $Q = 0$ to Q_{max}. Its unmistakable signature thus present in the data is very likely to be captured by the least-squares analysis. Detecting thinner layers is progressively harder. One may be able to argue that under favourable conditions (*e.g.* good contrast with other layers) a layer of thickness $(1/2)t_{min}$ can be detected. However, a similar claim for a layer of thickness, say, only 10% of t_{min} will be met with scepticism. It would be analogous to claiming a real-space resolution much better than the inverse of the maximum $\sin\theta/\lambda$ cutoff for a crystal structure analysis.

It is therefore surprising, especially for those with a background in crystallography, to learn that neutron reflectometry under suitable conditions can genuinely detect layers that are much thinner than $2\pi/Q_{max}$. We will herein refer to these as ultra-thin films (UTFs). Private communications suggest a horde of examples exist in the literature but this author is familiar with only two: namely Steitz *et al.* (2003) and Unsworth *et al.* (2006). In both cases the UTF is sandwiched between two contrast-matched media, *i.e.* two media whose scattering-length densities are equal or made equal by isotopic replacement. Steitz *et al.* (2003) studied the formation of nanobubbles at the interface of water and polystyrene, and came close to providing a fully satisfactory qualitative description. Water in this case is D_2O, which is nearly perfectly contrast-matched to deuterated polystyrene (dPS). The authors pointed out that because of the contrast matching the dPS/D_2O interface is invisible to neutrons. However, in the presence of nanobubbles, the scattering-length density at the interface will have a local minimum, and thus will become visible. While this argument is not wrong, it leads to several questions. For instance, the local minimum the authors discuss is actually made up of two interfaces, dPS/bubble and bubble/D_2O. Since these two interfaces are spatially very close ($<<2\pi/Q_{max}$) is it reasonable to say that they could be resolved from each other? If they are not resolved, why should we see their effect? This brings us back to the lack of resolution, the question that caused the dilemma in the first place. Another follow-up question would be: what aspect of measured reflectivity carries the information about the UTF? Do we detect it through a mathematical peculiarity in the critical region (around Q_c) or is the information over the entire reflectivity curve? Finally, can we really trust the scattering-length density of the UTF determined this way?

We will hereby develop an intuitive way of thinking to provide answers for the foregoing questions. With contrast matching we know it is indeed possible to detect UTFs. This possibility will be first demonstrated with reflectivity calculations for hypothetical models. We will then present an argu-

ment in terms of phase-vector diagrams as a way of qualitatively explaining the calculated reflectivity. Finally, we will show that the scattering-length density of the UTF thus determined, in relation to that of the contrast-matched media, is unique.

2. Simulation with hypothetical models

We will imagine a scenario where one wishes to study a polymer film in an aqueous environment. The film will be adsorbed on the surface of a metal layer, itself deposited (usually by sputtering) on polished bulk single-crystal Si. The bulk Si is typically a circular slab, 100 mm in diameter and 12 mm thick. Depicted edge-on in Fig. 1, Si serves as the medium of propagation for the neutron beams. This arrangement is commonly used in neutron reflectometry because it allows the beams to be entirely on the Si side of the metal/polymer system, providing unlimited free space on the other side to set up the aqueous environment. Single-crystal Si is highly transparent to thermal and cold neutrons – attenuation through 100 mm Si is only 15–20%.

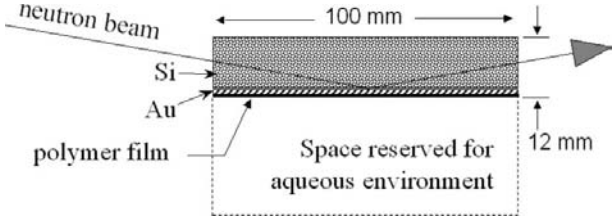

Figure 1
A schematic view of neutron reflectometry designed to study a polymer thin film, tethered to gold on one side and exposed to a liquid medium on the other side. A circular slab of single-crystal Si, shown edge-on, serves as the supporting substrate as well as the propagating medium for the neutron beams.

For simulations, we will assume that the metal is a 400 Å thick gold layer. Its surface will be covered with tethered polymers, to be exposed to an aqueous solution. Most polymers, due to the negative scattering length of H, have scattering-length density in the 10^{-7} Å^{-2} range instead of the 10^{-6} Å^{-2} range common for hydrogen-free materials. This, combined with the desire to reduce the incoherent scattering background, usually leads to the use of D_2O instead of H_2O for the aqueous medium. One could further improve the sensitivity to the polymer layer by using a D_2O/H_2O mixture (DHM) contrast matched to Au (required ratio = 73:27 by volume, *i.e.* mostly D_2O). The rationale is that the interface between Au and the DHM would be invisible (or nearly invisible) to neutrons in the absence of the polymer. Detection of the presence of a thin polymer layer can then be much easier.

Fig. 2 is the calculated reflectivity for the geometry of Fig. 1 [carried out with the *PARRATT32* software (Braun, 2003)]. We assume for the moment that there is no polymer layer on the gold surface and that the space on the other side is air. Such a 'dry' scan is usually measured as part of an experiment to characterize the substrate. In the sequence encountered by the incident neutrons, the interfaces producing partially reflected beams are Si/Au and Au/air. The coherence between the two beams leads to the interference pattern or Kiessig fringes with a periodicity of $\Delta Q = 2\pi/400 = 0.0157$ Å^{-1}.

Fig. 3 is the calculated reflectivity with the reserved space in Fig. 1 filled with DHM contrast matched to Au. Now that the sample consists of only one interface detectable by neutrons, the Si/Au interface, Kiessig fringes have disappeared and the reflectivity curve follows the Fresnel equation.

Fig. 4 shows the calculated reflectivity if a 3 Å thick polymer layer is present between Au and the DHM. Kiessig fringes reappear with the periodicity $\Delta Q = 0.0157$ Å^{-1}, attesting that the detection of the polymer layer is possible. The 3 Å thick

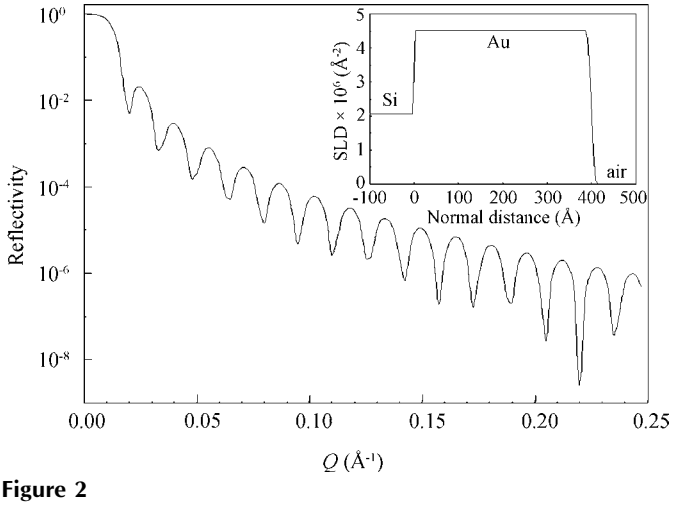

Figure 2
The calculated reflectivity of the Si/Au/air multi-interface system shown in the inset. Si and air are the initial and the final propagation media for the incident neutron beam. Scattering-length density is abbreviated as SLD.

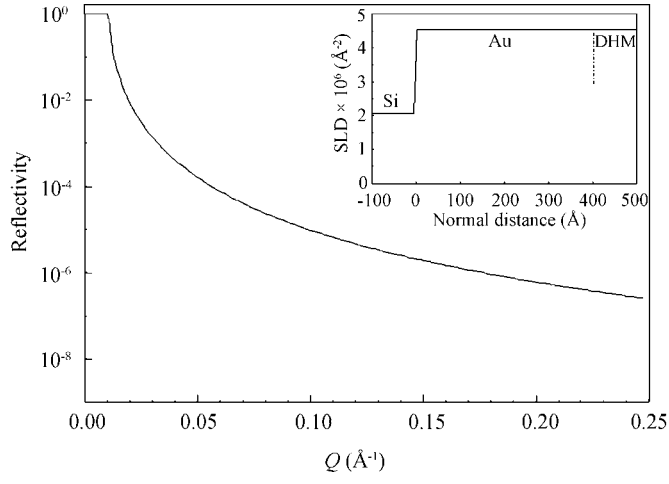

Figure 3
The calculated reflectivity of the Si/Au/DHM system where the final medium, DHM, is the D_2O and H_2O mixture contrast-matched to Au. Hence the interface between Au and DHM is invisible to neutrons (the dashed vertical line in the inset).

layer is a UTF, since it is much thinner than $2\pi/Q_{max}$ adopted for the simulated reflectivity curve.

3. Qualitative representation

The Kiessig fringes in Fig. 2 are from interference between the beams reflected at the Si/Au and Au/air interfaces, where the amplitude of each reflected wave is proportional to the contrast at the corresponding interface j ($j \geq 2$ for interference to occur). However, unlike for standard crystallography, the mathematical expression for resultant amplitude is not a simple sum of terms $f_j \exp(i\mathbf{Q}\cdot\mathbf{r}_j)$. Given by dynamical scattering theories such as by Parratt (1954), the expression consists of quantities that are monotonically decreasing with increasing Q and phase factors that become $\exp(iQd_j)$ if Q is significantly larger than Q_c, where d_j is the normal distance of the jth interface from a suitably chosen origin. Since the reflectivity modulations beyond Q_c arise solely from these phase factors, we can discuss the interference in terms of phase-vector diagrams. This representation will lead to correct predictions about the positions of the local reflectivity maxima and minima in Q space ($Q >> Q_c$), but does not in any way yield the absolute value of the reflectivity.

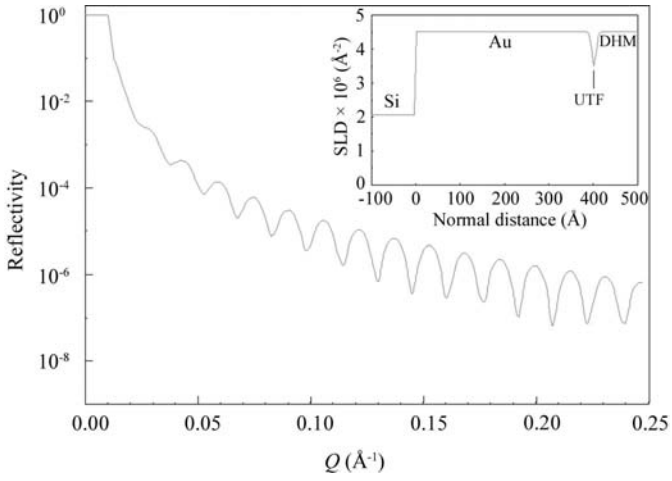

Figure 4
The calculated reflectivity of the Si/Au/UTF/DHM system.

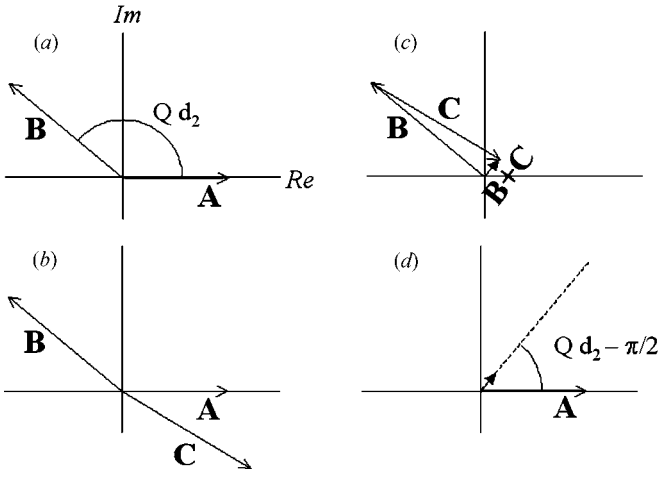

Figure 5
Phase-vector diagrams representing the beams reflected at the interfaces of (*a*) the Si/Au/air system and (*b*) Si/Au/UTF/DHM. Part (*c*) depicts the sum of the phase vectors **B** and **C**, while (*d*) represents the interference between **A** and **B** + **C**.

Fig. 5(*a*) shows the phase vectors representing beams reflected at the Si/Au and Au/air interfaces (Fig. 2). Vector **A** for the first interface is along the real axis, since we have chosen the position of this interface to be zero. The phase of vector **B** is then Qd_2, where d_2 is the thickness of the second medium, Au (we are here following Parratt's notations). The resultant vector **A** + **B** is at a local maximum if **A** and **B** are in phase, and at a local minimum if the two vectors are out of phase.

Fig. 5(*b*) shows the phase vectors corresponding to the layer profile of Fig. 4. Vectors **B** and **C** represent the interfaces Au/UTF and UTF/DHM. They are of equal magnitude but are approximately out of phase since the scattering-length-density gradient at the two interfaces is of the opposite sense. In the limit of the UTF thickness going to zero, **C** would be exactly out of phase with **B**. The phase of **C** is shown slightly more than π ahead of **B** because of the finite thickness of the UTF. The sum **A** + **B** + **C** represents the resultant reflected amplitude. **B** + **C** is a small but finite vector whose phase differs from **B** and **C** by approximately $\pi/2$ (Fig. 5*c*). The reflectivity modulation of Fig. 4 arises from the interference represented by **A** + (**B** + **C**) as depicted in Fig. 5(*d*).

The $\pi/2$ phase shift of (**B** + **C**) from the average phase of **B** and **C** has an important consequence: although the periodicity in Fig. 4 is the same as in Fig. 2, the maxima and minima should appear shifted by a quarter of a period. This expected shift is demonstrated in Fig. 6, where the reflectivities of Figs. 2 and 4 are plotted as the bold solid curve and the dashed curve after being divided by the reflectivity of Fig. 3. The division removes

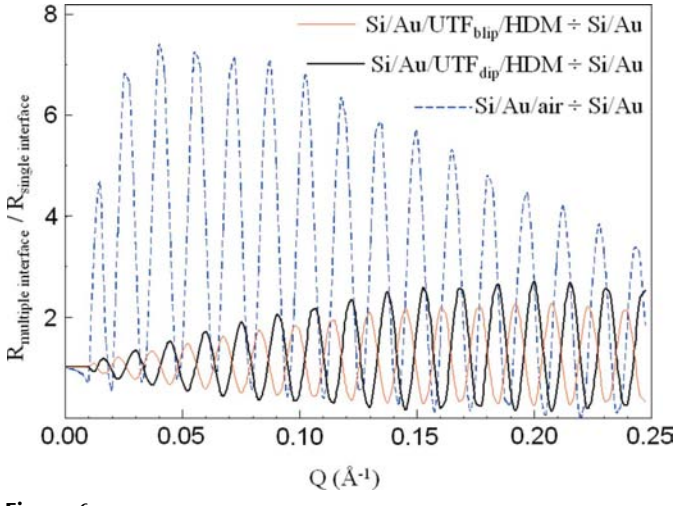

Figure 6
Reflectivities R of Figs. 2 and 4 divided by that of Fig. 3, plotted as the dashed and the bold solid curves, respectively. The lighter solid curve is calculated in the same way as for the bold curve, except that the scattering-length density of the UTF is assumed to be higher, rather than lower, than the scattering-length density of its adjacent neighbours.

the monotonic decrease due to the Fresnel equation, making the comparison of the peak positions easier. It is striking to consider what would happen if the scattering-length density of the UTF is higher than that of its adjacent media, *i.e.* a blip instead of a dip in the inset of Fig. 4. Then the directions of both **B** and **C** would reverse, changing the sign of the $\pi/2$ phase shift of (**B** + **C**). For this scenario the peaks shift in the opposite direction, as shown by the lighter solid curve in Fig. 6.

It is worth pointing out that although the phase-vector diagrams are for idealized sharp interfaces (a single well defined vector for each interface), the simulations presented earlier were carried out with roughened interfaces on either side of the UTF. This is evident in the inset of Fig. 4, where the UTF dip has a sharp tip (not a square box) since it is formed by two back-to-back sigmoid functions of 5 Å width. Considering that the UTF they model is only 3 Å thick, these are indeed very rough interfaces. Even if we invoke the possible effects of correlated or conformal roughness [see, for example, Tolan (1999)] none is known to give the $\pi/2$ phase shift as seen in Fig. 6. Experimentally, those such as Steitz *et al.* (2003) prove unequivocally that practical issues, *e.g.* interface roughness or less-than-perfect contrast matching, are *not* detrimental to the study of UTFs with reflectometry.

4. Conclusion

We have demonstrated qualitatively the principle of the detection of a UTF when it is placed between two contrast-matched media. The information is conveyed by the entire reflectivity curve, not just a special part of the Q space, and the determination of the scattering-length density of the UTF is unambiguous and reliable.

Appreciation of this rather surprising capability of reflectometry goes back many years. At the 1994 Materials Research Society Symposium, Majkrzak (1995) presented an example where the existence of a feature, only 5 Å in overall thickness, on the surface of a hypothetical ~40 Å thick free-standing film would lead to easily detectable changes in specular reflectivity measured out to $Q_{\max} = 0.2$ Å^{-1}. This example also involves contrast matching, since a free-standing film is a layer sandwiched between two media of zero scattering length. The changes, however, are not so simple to explain qualitatively, as the scenario considered is far more complex than ours: the surface feature considered was made of three closely spaced interfaces (instead of two), and contrast matching is across the entire layer system (not just across the surface feature). Nevertheless, Majkrzak (1995) provided an early demonstration (probably the first) of the potential reflectometry has as a uniquely powerful tool in the study of extremely thin films.

The extreme sensitivity of neutron reflectometry to very thin films under special conditions highlights the importance of sample handling. For a noble metal such as Au, known not to form a passive oxide layer, coverage even by a monolayer of hydrocarbons may be sufficient to give a measurable signal. What one thinks to be the 'signal' could turn out to be 'noise' from a dirt layer.

The author thanks Kan Tun for help in preparing the manuscript, and Dr C. F. Majkrzak for kindly reading through the preprint and encouraging me to proceed with the publication of the paper.

References

Braun, C. (2003). *PARRATT32.* Version 1.5. Berlin Neutron Scattering Center, Germany.

Majkrzak, C. F. (1995). *Fundamentals of Specular Neutron Reflectometry*, Materials Research Society Symposium Proceedings, Vol. 376, *Neutron Scattering in Materials Science II*, edited by D. A. Neumann, T. P. Russell & B. J. Wuensch, pp. 143–156. Warrendale: Materials Research Society.

Parratt, L. G. (1954). *Phys. Rev.* **95**, 359–369.

Steitz, R., Gutberlet, T., Hauss, T., Klösgen, B., Krastev, R., Schemmel, S., Simonsen, A. C. & Findenegg, G. H. (2003). *Langmuir*, **19**, 2409–2418.

Tolan, M. (1999). *X-Ray Scattering from Soft-Matter Thin Films*. Berlin: Springer.

Unsworth, L. D., Tun, Z., Sheardown, H. & Brash, J. L. (2006). *J. Colloid Interface Sci.* **296**, 520–526.